PAPER • **OPEN ACCESS**

Online Inspection Method of Defect Dimension of Stainless Steel Precision Blanking Sheet Contour

To cite this article: Weichao Shi *et al* 2019 *IOP Conf. Ser.: Mater. Sci. Eng.* **490** 052009

IOP Conf. Series: Materials Science and Engineering **490** (2019) 052009 doi:10.1088/1757-899X/490/5/052009

Online Inspection Method of Defect Dimension of Stainless Steel Precision Blanking Sheet Contour

Weichao Shi[1], Jianming Zheng [1,*] and Lijie Wang[1]

[1]School of Mechanical and Instrumental Engineering, Xi'an University of Technology, Xi'an, China

*Corresponding author e-mail: zjm@xaut.edu.cn

Abstract. In this study, a new method of online inspection of contour defects is proposed for stainless steel precision blanking sheet to address problems in the use of the current method to obtain detect information: the recognition system is complex, and the measurement error of defect dimension is large. The images of defect blanking sheet are obtained by the established image collection system. The results of image analysis show that the defect contour of blanking sheet has the correspondence and similarity characteristics. An improved sequential similarity detection algorithm and the measurement algorithm are developed. The measurement experiments show that the online inspection system is stable and reliable, and the maximum measurement error is 0.0362mm. The results of this study will lay a foundation for the online inspection of precision machining.

1. Introduction

The stainless steel sheet, which was processed by precision blanking, is a corrosion resistant part with a thickness less than 1mm, and has strong plasticity and toughness. In the process of precision blanking, cutting edges wear, which was caused by friction between stainless steel band and the blanking, was the main failure mode of the blanking die [1]. And it was easy to cause the wear defect of sheet contour, which seriously affected the quality of stainless steel sheet. At present, the inspection method based on machine vision technology was widely concerned [2-5], researchers have used the technology to solve the problem of online inspection of the contours of precision blanks [6-12]. However, the most of the defect recognition system is complex and the error of defect dimension is large. Therefore, it is necessary to establish a new online inspection of the blanking sheet to meet the rapid and accurate inspection requirements.

To solve the above problem, the online inspection method of precision blanking sheet was proposed. The image collection system was established, and obtained the images of defect blanking sheet. According to the correspondence and similarity characteristics of defect caused by the same cutting edges wear, an improved sequential similarity detection algorithm was established to confirm contour defects, and the measurement algorithm of contour defect dimension was developed. Therefore, the method of online inspection can not only identify the defect, but also measure the defect size.

2. Image collection of blanking sheet

2.1. Image collection system

The image collection system mainly consists of collection device and auxiliary device. Collection device includes light source, industrial CCD camera, image collection card and computer. Auxiliary device includes conveyor, blanking buffer device, calibration mechanism, mobile platform, etc. The industrial CCD camera adopts the DFK series 42BUC03 produced by the Imaging Source Company, the maximum resolution is 1280 pixels × 960 pixels, the pixel dimension is 3.75μm. The image acquisition card adopts the DH-VT110 with PCI bus interface, which supports multiple upper computer development software and could collect multi-mode image. The mobile platform adopts 550 multi-function precision cross slippery platform of milling machine, which is 255mm x 130 mm, configured with column and base. Industrial CCD camera was mounted on a mobile platform. The principal optic axis of the camera lens was perpendicular to the conveyor. The mobile platform can move along the X direction, Y direction and Z direction. The image acquisition card is installed in the PCI expansion slot of the computer, as shown in Fig.1.

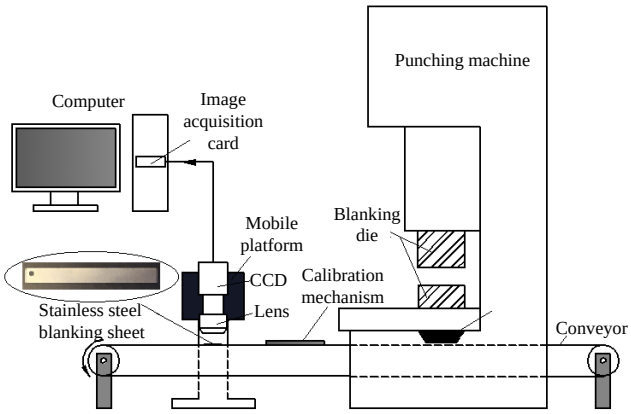

Figure 1. The image collection system.

Before the inspection system start, the location of the mobile platform was adjusted to achieve the parameters setting of the camera. After the system start, the blanking sheets are arranged through the blanking buffer device mounted on the feeding port of punching machine, and fell on the conveyor one by one. The calibration device installed on both sides of the conveying mechanism makes the blanking sheet at the center of the conveyor. CCD camera is used to collect the image of the sheet and transmit image to computer.

2.2. Image of defect blanking sheet

According to material forming theory, the location of cutting edges wear will not change under the action of blanking force, but the wear area will increase. Therefore, the defects caused by the same wear are similar, which is also verified by a large number of sheet defect images collected in the experiment. The image of defect blanking sheet is shown in Fig.2.

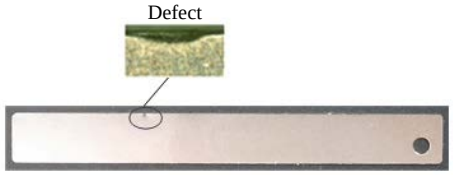

Figure 2. The contour defect of blanking sheet.

From the collection image, it can be seen that the defect area located on the edge of the blanking sheet were collection of low grayscale pixels and occupied a very small proportion in the image of the blanking sheet. The contour of the defect area is irregular and has similarity. As the cutting edge wear increases, the defect area is increasing.

3. Online inspection algorithm for contour defect of blanking sheet

3.1. Defection recognition

According to the characteristics of defect similarity, the recognition method of contour defect is proposed based on Sequential Similarity Detection Algorithm (SSDA).The specific process as follows:

（1）Before the system work, the images of defect-free blanking sheet are collected and adjusted. Taking the center of sheet area ($a \times b$) as the origin of the coordinate system, the gray image of region ($(a+10) \times (b+10)$) is extracted, and the extraction image is set as the standard image.

（2）As the system working, the images of blanking sheet, which to be matched, are collected and adjusted.

（3）Compared the gray average of each rank between the matching image and the standard image. The location of the change area of the grayscale is recorded, and the region image is extracted as template image.

（4）Based on SSDA algorithm, the template image is matched with other matching images. If there is a similar region of template image in other matching images, which the location is consistent, the region is the defect area.

3.2. Defection measuring

3.2.1. Image segmentation of defect area. Due to the few pixels and low density in the defect area, the threshold obtained by the global threshold method cannot separate the target area from the background. Therefore, the defect area is divided into several sub-regions, which are composed of the defect sub-region and the background sub-region. The dimension of the sub-region is (R×R), as shown in Fig.3. The upper area including defect sub-region, the lower area includes background sub-region.

Figure 3. Defect area partition map.

As can be seen from Figure 3 that the sub-regions of different positions have different gray variance, and the fluctuation of gray variance in the lower 12 sub-regions is very small. The fluctuation of gray variance of the 4 sub-regions on the left side of the upper row is small, which is basically equal to the gray variance of lower row. However, the variation of gray variance in the other eight sub-regions is significant, indicating that the defect exists in these eight sub-regions. Therefore, it can be excluded from the defect sub-region in the defect area. According to the default segmentation threshold of the defect sub-region, the Otsu algorithm is used to divide the sub-regions, and the binary image of the defect area is shown in Fig.4.

Figure 4. The binary image of the defect area.

3.2.2. The defect area connection. The Region Seeds Growing (RSG) algorithm is used to solve the problem of the regional discontinuous phenomena of sub-regions with smaller gray variance. The RSG algorithm use a low gray value pixel as a seed, and four neighbourhood extensions around the seed are carried. According to the rule that the absolute value of the gray level difference of the adjacent pixels is less than the specified threshold, whether the pixels around the seed belong to the seed region is determined, and the defect connection can be achieved by connecting the pixels in the region. The connection image of defect area is shown in Fig.5.

Figure 5. The connection image of defect area.

3.2.3. Defect image thinning and measurement. The binary image can be transformed into pixel image with a single width of 1 using the skeleton algorithm, as shown in Fig.6. Then, the system is calibrated, and the calibration factor is obtained. The true dimension of the defect contour is calculated according to the dimension of the defect contour pixel. The calculation formula is as follows:

$$L = L_p \times A \quad (1)$$

Where, L represents the true dimension of the defect contour (*mm*), L_p represents the pixel dimension of the defect contour (*pixel*), and A represents the calibration factor (*mm/pixel*).

Figure 6. The skeletonization image of defect.

4. Experiment

To verify the online detection method of the defect contour dimension of the blanking sheets, the experimental device is established, using a company produced J23 series punching machine and thickness 0.3 mm, width 120 mm of SUS304 stainless steel belt, as shown in Fig.7.

Figure 7. Experimental equipment.

4.1. Calibration of measurement system

According to the dimensional accuracy requirement of blanking sheet, the edge of the gauge block was measured using the gauge block of 1 level nominal length of 8mm as the calibration. The gage block placed in system is shown in figure 2, 15 images of the gauge block were obtained through the rotation of the conveyor. Therefore, the pixel points of the calibration dimensional can be calculated according to the defect measurement algorithm presented in section, as shown in Table 1.

Table 1. Measurement data of calibration dimensional.

Numbers	1	2	3	4	5	6	7	8	9	10	11	12	13	14	15
Pixel points	96	99	97	95	99	96	97	98	95	97	96	96	97	99	98
Average point								97							

From the data in Table 1, we can calculate that the average pixel points of the calibration dimensional is 97.1. The calibration factor is 0.0823mm/pixel, and the maximum repeatability measurement error is 1.6%. The measurement accuracy of the system can meet the measurement requirements of the defect dimensional.

4.2. Units Experimental result

In the process of blanking experiment, there was no wear defect sheet in the initial stage. With the blanking number to 5312 times, an unknown grayscale set appears on the image of the blanking sheet

edge, and the grayscale was determined to be wear defect by the algorithm of defect recognition algorithm.

The defect area of 15 blanking sheet is measured respectively using online defect inspection algorithm and the measuring device of VOG - 25 series image dimensional. The long sides of the blanking sheet set for the X, the short side for the Y, The measurement error of two kinds of measuring methods was calculated, the measurement results are shown in Table 2.

Table 2. Measurement data of defect dimensional.

Numbers	Inspection system (mm)		Measuring device (mm)		Measurement error (mm)	
	X	*Y*	*X*	*Y*	ΔX	ΔY
1	1.7407	0.4254	1.7721	0.4512	-0.0314	-0.0258
2	1.7454	0.4213	1.7728	0.4521	-0.0274	-0.0308
3	1.7443	0.4212	1.7692	0.4522	-0.0249	-0.0310
4	1.7456	0.4252	1.7737	0.4581	-0.0281	-0.0329
5	1.7411	0.4209	1.7710	0.4498	-0.0299	-0.0289
6	1.7423	0.4211	1.7726	0.4561	-0.0303	-0.0350
7	1.7417	0.4266	1.7746	0.4578	-0.0329	-0.0312
8	1.7436	0.4288	1.7783	0.4546	-0.0347	-0.0258
9	1.7422	0.4232	1.7681	0.465	-0.0259	-0.0418
10	1.7441	0.4207	1.7748	0.4476	-0.0307	-0.0269
11	1.7451	0.4287	1.7776	0.4568	-0.0325	-0.0281
12	1.7512	0.4307	1.7723	0.4576	-0.0211	-0.0269
13	1.7468	0.4207	1.7754	0.4471	-0.0286	-0.0264
14	1.7513	0.4354	1.7847	0.4634	-0.0334	-0.0280
15	1.7525	0.4367	1.7887	0.4622	-0.0362	-0.0255

It can be seen from the measurement results in Table 2 that the measurements of the vog-25 series image measuring device is larger than that of the Inspection system, this is mainly due to the error of the calibration factor of the two measurement systems. The maximum measurement error in the X direction is 0.0362mm, and the maximum measurement error in the Y direction is 0.0329mm, all of which are within the allowed measurement error. The measurement results show that the Inspection system is stable and reliable and can meet the requirements of online measurement.

5. Conclusion

According to the machine vision technology, the images of blanking sheet were obtained using the established collection system, and the characteristics of the images of defect blanking sheet were analyzed. The SSDA detection algorithm was improved to improve the accuracy of defect recognition, and the measurement algorithm was developed based on the image processing techniques. The measurement errors between the results of the online inspection and the measuring device were analyzed. The maximum measurement error is 0.0362mm, which verified the accuracy and reliability of the proposed method.

Acknowledgments

This work was financially supported by Natural Science Foundation Research Project of Shaanxi Province fund.

References

[1] T.J. Liu, Size parts defects and elimination methods, Chongqing University Press, Chongqing, 1988.
[2] Y. Li, G.l. Hua, Precision measurement technology, China Metrology Press, BeiJing, 2001.

[3] N.S.S. Mar, P.K.D.V. Yarlagadda, C. Fookes, Design and development of automatic visual inspection system for PCB Manufacturing, Robotics and Computer-Integrated Manufacturing 27 (2011) 949–962.

[4] S. Cubero, N. Aleixos, E. Moltó, J. Gómez-Sanchis, J. Blasco, Advances in machine vision applications for automatic inspection and quality evaluation of fruits and vegetables, Food Bioprocess Technol 4(2011) 487–504.

[5] T.-H. Sun, C.-C. Tseng, M.-S. Chen, Electric contacts inspection using machine vision, Image Vision Comput28 (2010) 890–901.

[6] Y. Gan, Q. Zhao, An effective defect inspection method for LCD Using active contour mode, IEEE Trans Instrum Meas62 (2013) 2438–2445.

[7] Henry Y.Y. Ngan, Grantham K.H. Pang, Nelson H.C. Yung, Automated fabric defect detection, Image Vision Comput29 (2011) 442–458.

[8] Kim T-H,Cho, Park SH, Visual inspection system for the classification of solder joints, Pattern Recogn32 (1999) 565–575.

[9] A Bhuvanesh,MM Ratnam. Automatic detection of stamping defects in lead frames using machine vision: Overcoming translational and rotational misalignment. The International Journal of Advanced Manufacturing Technology32 (2007)321201-1210.

[10] Y Wang, C Liu.The research of stamping workpiece detection algorithm based on digital image processing, Journal of Computational Information Systems10(2014) 6101-6107.

[11] D La, Inspection of metallic stamped parts using an image fusion technique, Intelligent Manufacturing Systems40(2007) 177-182.

[12] R.Wang, X.D. Zheng, D.N.HE, Artificial Neural Network Based Expert System for Diagnosing of Blanking Parts'Defects, Journal of Shanghai Jiaotong University35(2001)2001977-80.